Experimental demonstration of a collinear triple pulse grazing-incidence pumping scheme for a transient collisional pumped x-ray laser

2016 J. Phys. B: At. Mol. Opt. Phys. 49 215601

(http://iopscience.iop.org/0953-4075/49/21/215601)

IOP Publishing Journal of Physics B: Atomic, Molecular and Optical Physics
J. Phys. B: At. Mol. Opt. Phys. **49** (2016) 215601 (6pp) doi:10.1088/0953-4075/49/21/215601

Experimental demonstration of a collinear triple pulse grazing-incidence pumping scheme for a transient collisional pumped x-ray laser

S Künzel[1], G V Cojocaru[2], F Gärtner[3], B Aurand[4], L Li[5], D Ursescu[6], Ph Zeitoun[5], E Oliva[7], B Zielbauer[3], T Kuehl[3] and M Fajardo[1]

[1] GoLP/Instituto de Plasmas e Fusão Nuclear, Instituto Superior Técnico, 1049-001 Lisboa, Portugal
[2] National Institut for Lasers, Plasma and Radiation Physics, 409 Atomistilor Str., PO Box MG-36, 077125 Bucharest, Romania
[3] GSI Helmholtzzentrum für Schwerionenforschung GmbH, Planckstr. 1, D-64291 Darmstadt, Germany
[4] ILPP, Universität Düsseldorf, Germany
[5] Laboratoire d'Optique Applique, ENSTA-Paristech, CNRS, Ecole Polytechnique, UMR 7639, 828 Boulevard des Maréchaux, F-91128 Palaiseau, France
[6] Horia Hulubei National Institute for Physics and Nuclear Engineering, (IFIN-HH), ELI-NP Department, Reactorului str. 30, 077125, Magurele, Romania
[7] Instituto de Fusin Nuclear, E.T.S. de Ingenieros Industriales, Universidad Politécnica de Madrid, C/José Gutiérrez Abascal 2, E-28006 Madrid, Spain

E-mail: swen.kunzel@ist.utl.pt

Received 19 May 2016, revised 19 August 2016
Accepted for publication 16 September 2016
Published 10 October 2016

Abstract

We present a nickel-like Molybdenum x-ray laser (XRL) based on the transient collisional excitation scheme. Extending the double grazing-incidence pumping scheme to a triple pulse scheme with a nanosecond pre-pulse and two consecutive 3 ps pulses the output power of the XRL can be ~6 times increased compared to existing configurations, while using a relatively low total pump energy of 0.7 J. Additionally we show that this setup can be extended to a double stage, oscillator and amplifier stage, XRL.

Keywords: EUV, x-ray lasers, soft x-rays

(Some figures may appear in colour only in the online journal)

1. Introduction

Laser-plasma based XRLs have a high photon number [1] and spatial coherence [2] at soft x-ray wavelengths and are therefore suitable for applications as for example material science [3], holography [4] and plasma diagnostics [5]. Soft x-ray free-electron lasers [6] are large and only available in small numbers in contrary to XRLs, which fit in a laser laboratory-sized environment. High-harmonic generation (HHG) in noble gases requires less pump energy than XRLs [7] and provides a better brilliance [8] and transversal coherence [9] than XRLs but has the drawback of a lower photon number per pulse [10]. Consequently today the main goals in the development of XRLs is to relax the pump energy requirements and increase the quality of the output beam to achieve a higher beam brilliance. Using the transient collisional excitation scheme in combination with chirped-pulse-amplification lowered the pump requirements from kJ to ≈10 J [11]. The later developed grazing-incidence-pumping (GRIP) scheme allowed for saturated XRL emission at pump energies of ≈ 1 J [12] and therefore enabling higher repetition rates. The recently demonstrated double grazing-incidence-pumping scheme [13], in which the pulses for the plasma creation and heating are both collinear, shows a further

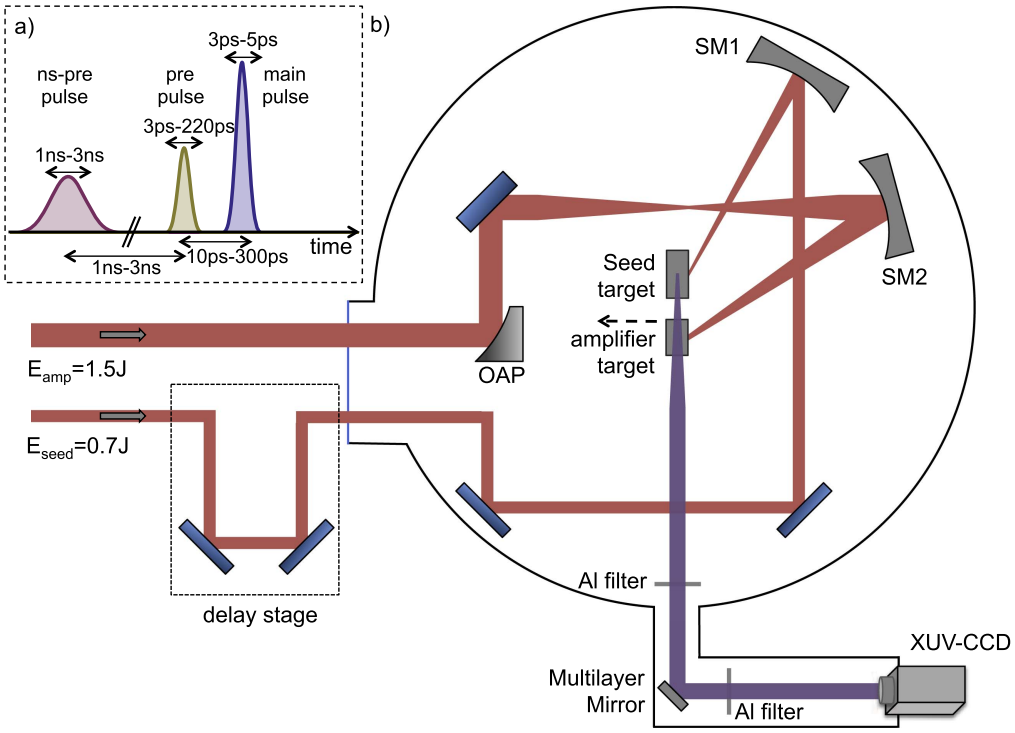

Figure 1. (a) shows the possible temporal configurations for the triple pulse structure. Pulse durations are the full-width-half-maximum values and pulse delays are given from peak-to-peak. (b) shows the experimental setup. (OAP = off axis parabola, SM = spherical mirror).

increase in XRL output energy and stability. The relatively low beam quality of XRLs results from the fact that XRL emission is based on amplified spontaneous emission, i.e. amplification of stochastic noise. This problem can be solved by seeding the XRL beam into a plasma amplifier, which increases significantly the photon number, coherence and brilliance [14].

We report on experimental results of a scheme using triple pulse grazing-incidence pumping (TGRIP). Simulations of this scheme were already carried out by Janulewicz and Kim [15] and the scheme was experimentally implemented by Ecker [16] and Zimmer [17]. TGRIP uses three collinear pulses to pre-form, create and heat a nickel-like molybdenum plasma. While published simulations and experiments use a ns-pre-pulse and a long pump-pulse of 200 ps followed by a shorter pulse, we achieve optimized conditions with a ns-pre-pulse and two consecutive pulses as short as 3 ps. Furthermore we show that the TGRIP scheme can be used without any modification in an oscillator-amplifier configuration.

2. Experimental setup

The experimental setup for single stage and double stage operation is shown in figure 1(a). The PHELIX laser [18] beam with diameter of 70 mm operated at a repetition rate of ≈ 0.006 Hz is clipped by a rectangle mirror that reflects $\approx 1/3$ of the total beam energy (2.2 J compressed) to the beam-line for pumping the seed target and $\approx 2/3$ of the beam energy to the beam-line for the amplifier target. A spherical mirror focuses the beam on an 80 μm wide and 5 mm long spot on the seed target with a GRIP angle of 28°. The focus on the amplifier target is achieved with a combination of a 45° off-axis parabola and a spherical mirror. In this configuration a line-focus with a reduced width can be achieved [19], which results in a 300 μm wide and 2 mm long focus with an angle of 68° between the target and incident beam. Each molybdenum target is mounted on a linear stage and the seed target has additionally a rotation stage to compensate for refraction of the XRL output. The horizontal separation of the targets is 20 mm. A 45° multilayer mirror with a reflectivity of 50% for 18.9 nm reflects the XRL output to a back-illuminated thinned CCD (Princeton Instruments PIXIS-XO 1024B) placed approximately 1 m after the amplifier target. A set of aluminum (Al) filters is used to stop IR radiation and to attenuate the XRL pulses before the CCD. The generation of the triple pulse structure (figure 1(a)) is described in [18] and [20].

3. Results

The XRL seed output is optimized without the amplifier target. The total pulse energy available for the seed target is 0.7 J compressed, which is divided between the ns-pre pulse, pre-pulse, and the main-pulse. The pulse energy of the ns-pre pulse is left constant at 0.15 J. After finding the best parameters for the seed target the amplifier is put in place and the temporal delay between the two beamlines is scanned.

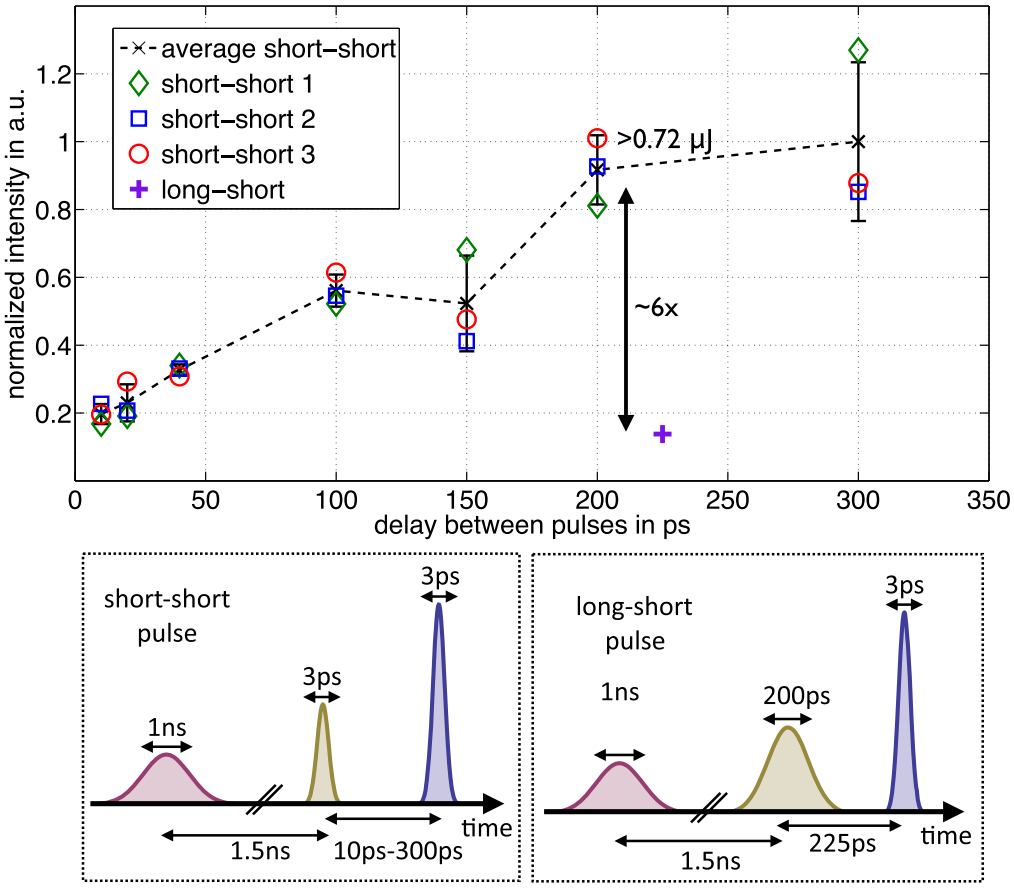

Figure 2. The upper graph shows the normalized XRL energy for different delays between the two pulses to create and heat the plasma. The intensities of the short–short pulse configuration are obtained from the average of three individual acquisitions. The long–short data point is the average of two individual acquisitions. The bottom figures show the temporal structure for the short–short pulse and long–short pulse configuration used in the experiment.

3.1. Single stage

The optimization of the seed target output is achieved by scanning the delays and pulse durations of the ns-pre-pulse, pre-pulse and main-pulse, and changing the energy splitting ratio between pre-pulse and main-pulse and changing the total pulse energy (figure 1(a)). Optimized conditions, in terms of photon counts and beam divergence, are found for a 30/70% energy splitting between pre-pulse and main-pulse and a duration of 1 ns for the ns-pre-pulse with a delay of 1.5 ns between the ns-pre-pulse and the pre-pulse and a delay of 200 ps between the pre-pulse and the main pulse. The duration of pre-pulse and main-pulse is equally short with 3 ps. Figure 2, shows the scan of the delay between the pre-pulse and main-pulse, while all other parameters are in optimized conditions. The data point for each delay is obtained by the average intensity of a series of three consecutive on a new target position. For comparison with existing results [16, 17] the duration of the main-pulse is changed to 200 ps at a delay of 225 ps between the pre-pulse and the main-pulse and is shown as the long–short data point in figure 2. The data point for the long–short pulse configuration is the average of two individual shots that have a difference in intensity of $<1\%$. As indicated in figure 2 changing to the long–short configuration results in 1/6 of the XRL energy achieved in the short–short configuration for pulse delays between 200 and 300 ps. Furthermore a decrease in beam quality in terms of divergence, as shown in figure 3, can be observed when switching to the long–short pulse configuration. The divergence of the short–short pulse configuration at a delay of 200 ps is 7.2 mrad $\times$ 8 mrad at the full-width-half-maximum (FWHM) of the intensity profile. In table 1 the presented XRL is compared to existing results using the TGRIP scheme. The maximum XRL pulse energy of Ecker [16] is 120 nJ and 2.2 μJ of Zimmer [17] for single stage XRL operation. The parameters for the long–short pulse configuration of the presented work are comparable to conditions of the two references. Assuming that the pulse energy reached in the long–short pulse configuration is comparable to the referenced values, we can estimate the short–short pulse configuration to reach a lower limit of 0.72 μJ for the pulse energy at 200 ps delay between pre-pulse and main-pulse. This is in agreement with the pulse energy of 0.87 μJ estimated from the CCD photon counts when the theoretical Al filter transmission [21] and a total aluminum oxide layer of 10nm per filter is considered [22]. The highest single stage XRL pulse energy is achieved with a delay of 300 ps, however the beam divergence is higher than at a delay of 200 ps (figure 3).

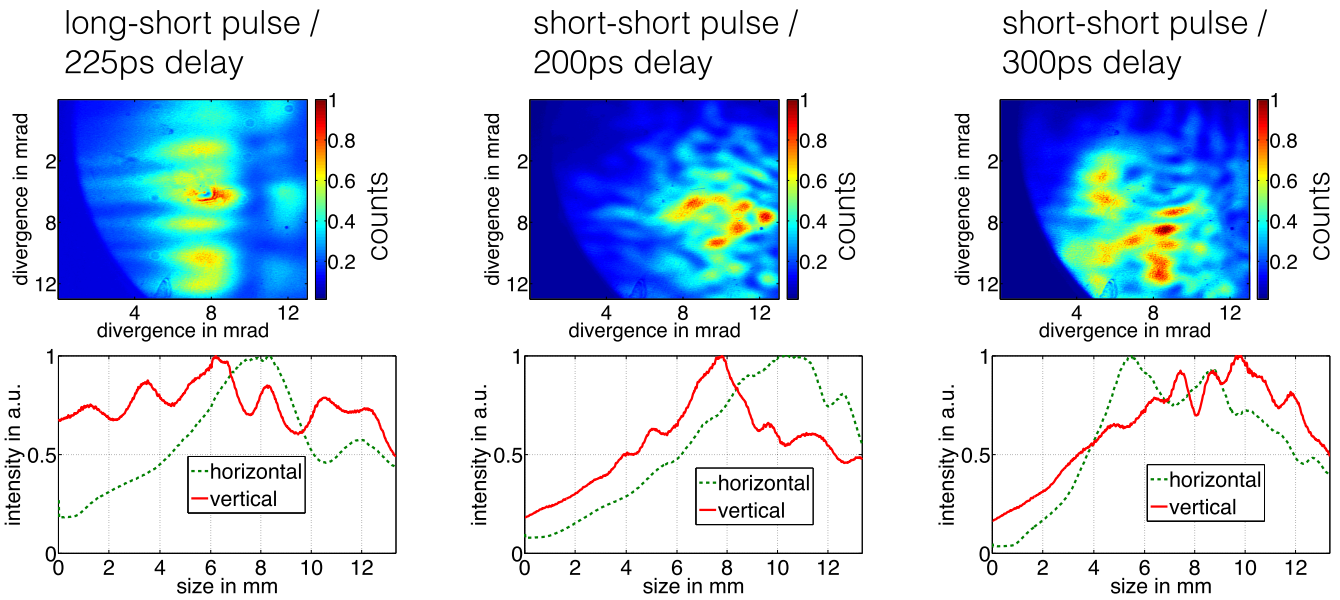

Figure 3. Normalized beam profiles and the corresponding integrations in the horizontal and vertical direction for different XRL pumping configurations: long–short pulse with 225 ps delay, short–short pulse with 200 ps delay and short–short pulse with 300 ps delay.

Table 1. Comparison of the peak intensity I_p (in W cm^{-2}) and pulse duration τ for different optimized XRL configurations.

Author and focus size	ns-pre pulse	Pre-pulse	Main pulse
Ecker [16]	$I_p = 2.0 \times 10^{10}$	$I_p = 8.0 \times 10^{10}$	$I_p = 2.0 \times 10^{13}$
5.0 mm × 90 μm (Mo)	$\tau = 1.7$ ns	$\tau = 200$ ps	$\tau = 2$ ps
Zimmer [17]	$I_p = 9.7 \times 10^{9}$	$I_p = 1.6 \times 10^{12}$	$I_p = 6.4 \times 10^{14}$
3.0 mm × 60 μm (Mo)	$\tau = 1.0$ ns	$\tau = 200$ ps	$\tau = 1$ ps
This work short-short	$I_p = 1.0 \times 10^{11}$	$I_p = 4.3 \times 10^{13}$	$I_p = 8.5 \times 10^{13}$
5.4 mm × 50 μm (Mo)	$\tau = 1.0$ ns	$\tau = 3$ ps	$\tau = 3$ ps
This work long–short	$I_p = 1.0 \times 10^{11}$	$I_p = 5.7 \times 10^{11}$	$I_p = 7.5 \times 10^{13}$
5.4 mm × 50 μm (Mo)	$\tau = 1.0$ ns	$\tau = 200$ ps	$\tau = 3$ ps

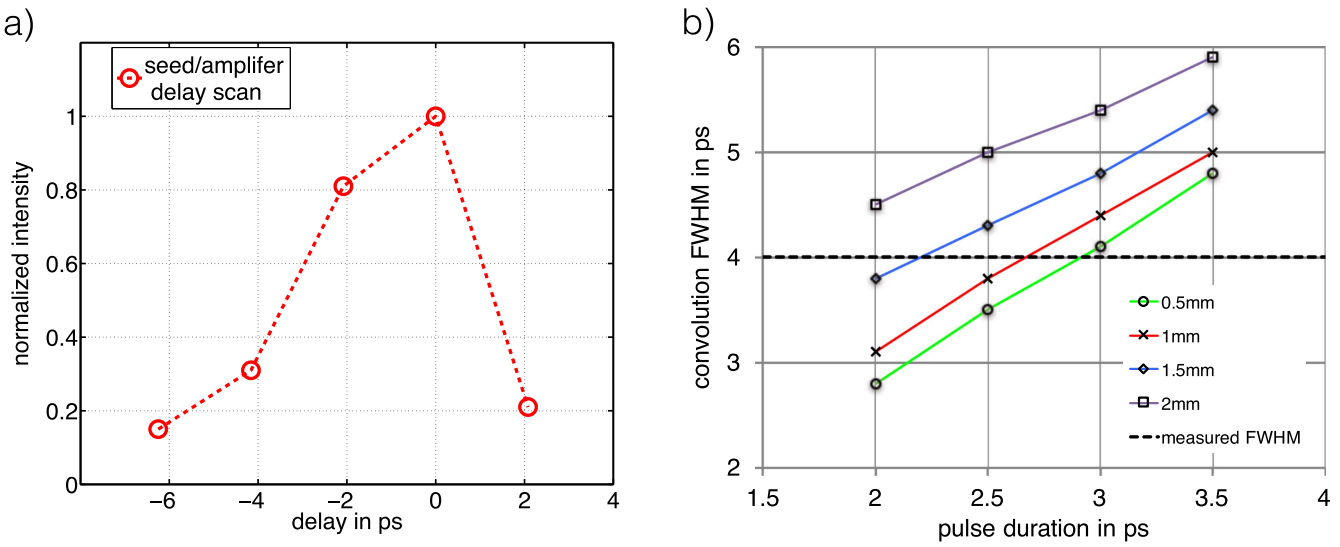

Figure 4. Results of the amplification dynamics with the double stage setup. (a) The experimental data is showing the delay scan between injection of the seed pulse and pumping of the amplifier target. The FWHM of the curve is ≈ 4 ps. (b) Results of the numerical simulations showing the calculated FWHM of the convolution for different seed/amplificiation pulse durations and effectively used target lengths with a traveling wave speed of 2.68 c for the excitation pulse.

3.2. Double stage

The optimized output of the seed target (short–short pulse configuration and 200 ps delay) is injected into the amplifier target, which is pumped by the same temporal pulse configuration as the seed target. The estimated beam-size of the seed output at the amplifier entrance is $\sim$300 μm. For finding best amplification conditions the delay between the pump pulses for the seed and amplifier target was scanned. The results are shown in figure 4. The main goal of the double-stage setup was to study the amplification dynamics and therefore the seed output was injected in the amplifier target without refocusing or imaging. This leads to a low spatial coupling efficiency of the amplifier which resulted in a photon count $\sim$50 times less than using the seed target alone. Figure 4(a) shows the amplifier output energy depending on the delay between the seed and amplifier pump pulses, which is the convolution of the seed pulse duration with the gain-lifetime of the amplifier target. The FWHM of the convolution is $\approx$ 4 ps. One can not infer the pulse and gain duration from the amplification scan alone. The speed of excitation traveling wave is $v_{\mathrm{TW}} = 2.68\,\mathrm{c}$ in the presented setup. Amplification along the whole amplifier target length of 2 mm would result in a minimum duration of 6.7 ps for the gain. However assuming that the seed pulse duration is not longer than the gain duration the FWHM of the convolution gives an upper limit of 4 ps for the gain duration. The measured convolution is broadened compared to a convolution measurement obtained at $v_{\mathrm{TW}} \approx \mathrm{c}$ due to the phase slippage between the traveling gain profile and seed pulse. Additionally the maximum distance a ray can travel in the gain-zone is limited by the gradient of the refractive index resulting from the electron density distribution. However data for the electron density is only available for the long–short pulse configuration [15]. Furthermore the effectively used amplifier target length is modified by rotation on the seed target to compensate induced refraction of the amplifier target to redirect the XRL pulses to the CCD. It is possible to retrieve an estimate for the seed and amplifier pulse duration if the same Gaussian line-shape is assumed for both. Numerical calculations were conducted for different amplifier target lengths to reproduce the experimental data of the convolution. The results are shown in figure 4(b). The experimental results are matched for a pulse duration between 2 and 3 ps. This is shorter than the value of 5 ps observed by Ecker [16] for a triple pulse scheme in a long–short pulse configuration. Compared to Ecker a $\sim$4 times higher peak intensity is used for the main pulse, which creates a higher electron temperature. This results in a faster collisional ionization of the Ni-like ions [23] and a shorter XRL pulse duration.

4. Conclusion and outlook

In conclusion we showed that in a pumping scheme with three pulses the XRL output can be further improved by using a ns-pre-pulse followed by two 3 ps pulses. All three pulses are collinear, which simplifies the experimental setup and pulse timing. The photon count can be increased $\sim$6 times compared to existing XRL pump pulse configurations.

In a pumping scheme with three pulses the formation of the plasma, the creation of the nickel-like state of the ions and heating of the electrons is decoupled. The output intensity depends on the number of lasing ions and consequently on the nickel-like abundance of the ions and the electron temperature for the collisional excitation. With identical heating pulses, both long–short and short–short configuration, have the same electron temperature. The lower gain with a long second pulse (200 ps) therefore suggests a less efficient nickel-like ion generation than a short pulse (3 ps).

The XRL can be extended to a double stage XRL using the same pulse configuration. First amplification dynamics measurements show a pulse duration between 2 and 3 ps and a gain factor of 6, which is also useful information for benchmarking simulations. Due to a low coupling efficiency the photon count in the double stage configuration is lower compared to the single stage output. This drawback can be compensated by imaging the seed target output on the entrance of the amplifier target and a rotation stage for the amplifier target for compensation of refraction. With this improvements we expect a decreased beam divergence and photon count above the level of the seed, which leads in total to a higher peak brilliance. In the single stage configuration an output of 7×10^{10} photons per shot with a relative bandwidth $\Delta\lambda/\lambda$ of 5×10^{-5} [16] was achieved which is competitive with other spatial coherent XUV sources. HHG driven by a 40 fs laser at 800 nm in argon has a relative bandwidth of 4×10^{-2} with 1.6×10^{8} photons per pulse for the 25th high-harmonic order [24]. The FLASH FEL can be tuned from 6.8 to 47 nm [25] and achieves in average $\approx 6 \times 10^{12}$ photons per shot in a relative bandwidth of 1×10^{-2}. It has to be noted that HHG has the ability to produce isolated pulses with attosecond duration using a few cycle driving lasers [26], which results in a relative bandwidth of 4×10^{-1}.

The presented results show the importance of collinear traveling amplified laser pulses for pumping XRLs. Newly developed diode pumped laser systems based on ytterbium-doped gain media [27] allow the amplification of several pulses due to high saturation fluence of the amplification media [28]. Using this new generation diode pumped lasers the efficiency and repetition rate of XRLs using several collinear excitation pulses can be further increased, while the pumping requirements for the laser are lowered.

Acknowledgments

We wish to thank the GSI PHELIX laser team for support of the experiment. This work was supported by the European Union's Horizon 2020 research and innovation programme under grant agreement no. 284464 Laserlab-Europe and grant agreement no. 665207 voxel. This work was also supported by FCT grant PTDC/FIS/112392/2009 and COST Action MP1203.

References

[1] Rus B *et al* 2007 Development and applications of multimillijoule soft x-ray lasers *J. Mod. Opt.* **54** 2571–83

[2] Nishikino M, Tanaka M, Nagashima K, Kishimoto M, Kado M, Kawachi T, Sukegawa K, Ochi Y, Hasegawa N and Kato Y 2013 Demonstration of a soft-x-ray laser at 13.9 nm with full spatial coherence *Phys. Rev.* A **68** 061802

[3] Mocek T, Rus B, Kozlová M, Polan J, Homer P, Juha L, Hájková V and Chalupský J 2008 Single soft x-ray laser-induced ablative microstructuring of organic polymer with demagnifying projection *Opt. Lett.* **33** 1087

[4] Trebes J, Brown S B, Campbell E M, Matthews D L, Nilson D G, Stone G F and Whelan D A 1987 Demonstration of x-ray holography with an x-ray laser *Science* **238** 517–9

[5] Da Silva L B *et al* 1995 X-ray lasers for high density plasma diagnostics *Rev. Sci. Instrum.* **66** 574

[6] Tiedtke K *et al* 2009 The soft x-ray free-electron laser FLASH at DESY: beamlines, diagnostics and end-stations *New J. Phys.* **11** 023029

[7] Christov I P, Zhou J, Peatross J, Rundquist A, Murnane M M and Kapteyn H C 1996 Enhanced high-harmonic generation using 25 fs laser pulses *Phys. Rev. Lett.* **77** 1743

[8] Kim H T, Kim I J, Tosa V, Lee Y S and Nam C H 2004 Bright high-order harmonic generation at 13 nm and coherence measurement *Appl. Phys.* B **78** 863–7

[9] Déroff L L, Salières P, Carré B, Joyeux D and Phalippou D 2000 Measurement of the degree of spatial coherence of high-order harmonics using a Fresnel-mirror interferometer *Phys. Rev.* A **61** 043802

[10] Takahashi E, Nabekawa Y and Midorikawa K 2002 Generation of 10 μJ coherent extreme-ultraviolet light by use of high-order harmonics *Opt. Lett.* **27** 1920–2

[11] Shlyaptsev V N, Nickles P V, Schlegel T, Kalachnikov M P and Osterheld A L 1994 Tabletop x-ray laser pumped with subnanosecond and picosecond pulses *Proc. SPIE* **2012** 111

[12] Keenan R, Dunn J, Shlyaptsev V N, Smith R F, Patel P K and Price D F 2003 Efficient pumping schemes for high average brightness collisional x-ray lasers *Proc. SPIE* **5197** 213–20

[13] Ecker B *et al* 2012 Gain lifetime measurement of a Ni-like Ag soft x-ray laser *Opt. Express* **20** 25391–9

[14] Zhao H Y *et al* 2014 High-brilliance double-stage soft x-ray laser pumped by multiple pulses applied in grazing incidence *J. Phys.: Conf. Ser.* **488** 142004

[15] Janulewicz K A and Kim C M 2010 Role of the precursor in a triple-pulse pumping scheme of a nickel-like silver soft-x-ray laser in the grazing-incidence-pumping geometry *Phys. Rev.* E **82** 056405

[16] Ecker B *et al* 2015 Double-stage soft x-ray laser pumped by multiple pulses applied in grazing incidence *J. Phys. B: At. Mol. Opt. Phys.* **48** 144009

[17] Zimmer D, Zielbauer B, Pittman M, Guilbaud O, Habib J, Kazamias S, Ros D, Bagnoud V and Kuehl T 2010 Optimization of a tabletop high-repetition-rate soft x-ray laser pumped in double-pulse single-beam grazing incidence *Opt. Lett.* **35** 450–2

[18] Bagnoud V *et al* 2010 Commissioning and early experiments of the PHELIX facility *Appl. Phys.* B **100** 137–50

[19] Ross I N, Boon J, Corbett R, Damerell A, Gottfeldt P, Hooker C, Key M H, Kiehn G, Lewis C and Willi O 1987 Design and performance of a new line focus geometry for x-ray laser experiments *Appl. Opt.* **26** 1584–8

[20] Kuehl T *et al* 2010 Progress in the applicability of plasma x-ray lasers *Opt. Lett., Hyperfine Interact.* **196** 233–41

[21] Henke B L, Gullikson E M and Davis J C 1993 X-ray interactions: photoabsorption, scattering, transmission, and reflection at $E = 50$–30000 eV, $Z = 1$–2 *At. Data Nucl. Data Tables* **54** 181–342

[22] Mitrofanov A V and Tokarchuk D N 1989 Fabrication of multilayer thin film filters on support screens and their properties *Nucl. Instrum. Methods Phys. Res.* A **282** 546–50

[23] Ochi Y, Kawachi T, Hasegawa N, Sasaki A, Nagashima K, Sukegawa K, Kishimoto M, Tanaka M, Nishikino M and Kado M 2004 Measurement of temporal durations of transient collisional excitation x-ray lasers *Appl. Phys.* B **78** 961–3

[24] Künzel S *et al* 2015 Shot-to-shot intensity and wavefront stability of high-harmonic generation *Appl. Opt.* **54** 4745–9

[25] Treusch R and Feldhaus J 2010 FLASH: new opportunities for (time-resolved) coherent imaging of nanostructures *New J. Phys.* **12** 035015

[26] Sansone G *et al* 2006 Isolated single-cycle attosecond pulses *Science* **314** 443–6

[27] João C P, Pires H, Cardoso L, Imran T and Figueira G 2014 Dispersion compensation by two-stage stretching in a sub-400 fs, 1.2 mJ Yb: CaF_2 *Opt. Express* **22** 10097

[28] Körner J, Reiter J, Hein J and Kaluza M C 2015 Temporal shaping of high peak power pulse trains from a burst-mode laser system *Appl. Sci.* **5** 1790–802